Inorganic Chemistry

Article

pubs.acs.org/IC

Interplay of Condensation and Chelation in Binary and Ternary Th(IV) Systems

Daniel K. Unruh, Joshua de Groot, Melissa Fairley, Anna Libo, Samuel Miller, and Tori Z. Forbes*

Department of Chemistry, University of Iowa, CB W374, Iowa City, Iowa 52242, United States

Supporting Information

ABSTRACT: Th(IV) readily undergoes hydrolysis and condensation in aqueous solutions to form polynuclear molecular species and the system becomes increasingly complicated when organic chelators or other metals are present in solution, leading to the formation of complexes with vastly different structural topologies. Five compounds containing binary and ternary Th(IV) complexes have been synthesized and structurally characterized using single-crystal X-ray diffraction, including $Na_4[Th_6O_2(C_{10}O_7N_2H_{14})_6]\cdot 20.5H_2O$ (Th_6hedta), $[Th(C_9O_6NH_{12})(H_2O)(NO_3)]\cdot 1.5H_2O$ (Th(ntp)), $[Th_2Al_8(OH)_{14}(H_2O)_{12}(C_6O_5NH_8)_4](NO_3)_6\cdot 17.5H_2O$ (Th_2Al_8heidi), $(C_4N_2H_{12})[Th_2Fe_2(OH)_2(H_2O)_2(C_6O_7H_4)_2(C_6O_7H_5)_2]\cdot 6H_2O$ (Th_2Fe_2cit), $(C_4N_2H_{12})[ThFe_2O(H_2O)_3(C_{11}O_9N_2H_{13})_2]\cdot 6H_2O$ ($ThFe_2$dhpta). Additional chemical characterization by infrared spectroscopy and thermogravimetric analysis provides information on the chelation by the organic ligands and thermal stability. These molecular complexes can be utilized to understand aqueous speciation in mixed-metal solutions and also provide information regarding contaminant adsorption on iron(III) and aluminum(III) oxide surfaces.

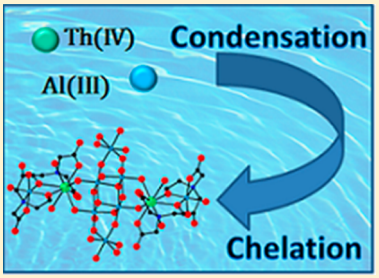

INTRODUCTION

Hydrolysis of metal cations readily occurs in aqueous solutions and can result in the condensation of soluble polynuclear precursors that impact the crystallization of oxide mineral phases and contaminant transport in environmental systems.[1−5] Under mildly acidic conditions, monomeric species, such as aqua complexes, tend to form, but upon addition of a base, condensation results in the formation of clusters with multiple metal centers.[3,6] It is likely that these polynuclear species are the building units or precursors to amorphous solid phases that can then undergo solid-state transformations to form crystalline materials.[5] Recent efforts to determine the structural nature of the precursor clusters is related to the desire to understand their control over the size, shape, and polymorph of mineral and nanoparticulate forms. In addition, these phases may be very important in environmental systems because they may constitute the primary components of iron(III) and aluminum(III) oxide colloids, which are important transport vectors for radioactive and heavy metal contaminants in surface and subsurface systems.[7]

A wide range of cations can undergo hydrolysis and condensation reactions to form molecular clusters in aqueous solutions, although many fall under the category of a hard Lewis acid.[4] Trivalent Al is an example of a relatively well-studied cation that readily condenses in aqueous solutions to form polynuclear clusters.[1,2,6,8−11] These clusters can vary from dimeric species to molecular clusters that contain 32 metal centers and exhibit different structural topologies based upon the rate and type of base that is added to the original solution.[12−19] Larger polynuclear species have been identified as the primary building blocks of amorphous aluminum hydroxide and a precursor to aluminum oxide mineral phases.[7,20−22] Other metal condensation products that have been previously investigated include Fe(III), Bi(III), Ga(III), Zr(IV), Hf(IV), Th(IV), U(IV), and U(VI) polynuclear species,[4,21,23−35] which are also currently being utilized as the building blocks for a wide range of oxide materials.[32,36−38]

While the condensation products of these isolated systems have been previously investigated, much less is known about the primary building blocks of heterometallic systems. The existence of these mixed-metal species and their influence on the chemical properties of the solution has been previously reported, but the structural details are lacking for many systems.[39−42] For example, aqueous solutions containing both Fe(III) and Th(IV) precipitate at higher pH values than for the individual components and exhibit greater solubility than their single-phase systems, but only one heterometallic species has been characterized by spectroscopic techniques.[39]

In environmental systems, the presence of natural organic matter and metabolites leads to additional complexities because organic molecules effectively compete with the condensation reaction leading to an interplay between chelation and formation of polynuclear clusters. Organic ligands can decrease the rate and extent of condensation via chelation of the metal center but can also effectively "cap" the polynuclear species, increasing the overall stability of the oxide in solution. Polycarboxylate ligands, such as citrate, are also prevalent in natural organic matter and can influence the speciation of metals in surface and subsurface environments.[22,43,44] Francis and Dodge[45] have observed that citrate will strongly bind to Fe(III), U(VI), and mixed-metal phases, effectively stabilizing

Received: September 25, 2014
Published: January 14, 2015

DOI: 10.1021/ic502313y
Inorg. Chem. 2015, 54, 1395−1404

Scheme 1

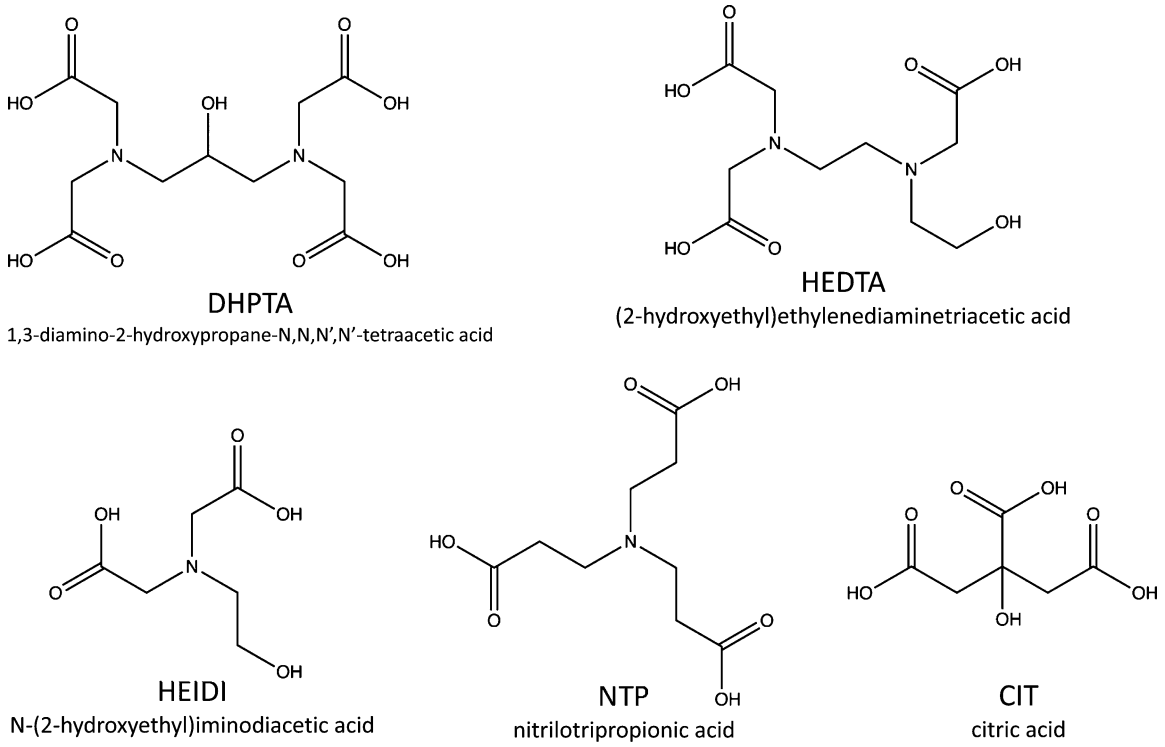

polynuclear species in solution. The formation of these binary and ternary species also results in significant changes in the rates of photo- and biodegradation, ultimately influencing the fate and transport of radionuclides in the environment.[46−48]

Our research group is interested in the interplay between condensation and chelation in both binary and ternary systems to provide an enhanced understanding of colloidal transport of radioactive contaminants in environmental systems. We have previously reported on hydrolysis of U(VI) and Al(III)/Th(IV) in the presence of polycarboxylates to provide structural information on molecular species that can occur in these regions.[31,49,50] In this work, we continue to extend our knowledge regarding hydrolysis in both Th(IV) and Th(IV)/(Fe(III),Al(III)) polycarboxylate systems (see Scheme 1) by synthesizing and characterizing five novel phases: $Na_4[Th_6O_2(C_{10}O_7N_2H_{14})_6]\cdot 28H_2O$ (Th_6hedta), $[Th(C_9O_6NH_{12})(H_2O)(NO_3)]\cdot 2.5H_2O$ (Th(ntp)), $[Th_2Al_8(OH)_{14}(H_2O)_{12}(C_6O_5NH_8)_4](NO_3)_6\cdot 57H_2O$ (Th_2Al_8heidi), $(C_4N_2H_{12})[Th_2Fe_2(OH)_2(H_2O)_2(C_6O_7H_4)_2(C_6O_7H_5)_2]\cdot 5H_2O$ (Th_2Fe_2cit), and $(C_4N_2H_{12})[ThFe_2O(H_2O)_3(C_{11}O_9N_2H_{13})_2]\cdot 3.5H_2O$ ($ThFe_2$dhpta). These particular ligands were chosen as part of a systematic study to investigate how the donicity of polycarboxylate ligand and the pH of the aqueous solution impacts the formation of a heterometallic clusters. In addition, the ligands have environmental relevance as both naturally occurring organic compounds and introduced metal chelators.

MATERIALS AND METHODS

Synthesis. $Th(NO_3)_4\cdot 5H_2O$, $Fe(NO_3)_3\cdot 9H_2O$, and $Al(NO_3)_2\cdot 9H_2O$ were purchased from Sigma-Aldrich, Alfa Aesar, and Acros Organic, respectively. The polycarboxylate ligands were purchased from Sigma-Aldrich (hedta, ntp), TCI (heidi), J. T. Baker (cit), and Acros (dhpta). All other chemicals were reagent grade and used without further purification.

Caution! *$Th(NO_3)_4\cdot 5H_2O$ is radioactive. The ^{232}Th in $Th(NO_3)_4\cdot 5H_2O$ is an alpha emitter and, like all radioactive materials, must be handled with care. These experiments were conducted by trained personnel in a licensed radiochemical research facility with special precautions taken toward the handling, monitoring, and disposal of radioactive materials.*

Th_6hedta. An aliquot of the solid hedta ligand (0.2782 g, 0.504 mmol) was added to 10 mL of 0.1 M aqueous Th(IV) nitrate solution (0.232 g, 1.0 mmol Th(IV)), and the pH was adjusted to 8.4 with 1 M NaOH. The resulting solution was stirred, and subsequent liquid−liquid diffusion with THF resulted in the formation of clear needles after 48 h. The crystals were rinsed with methanol and allowed to air-dry, and the percent yield of Th_6hedta was calculated as 72.1% based upon Th.

Th(ntp). Aluminum nitrate nonahydrate (0.94 mmol, 0.3519 g) and thorium nitrate pentahydrate (0.27 mmol, 0.1500 g) were dissolved in 2.5 mL of deionized water. A second aqueous solution containing the ntp ligand (0.0733 g in 2.5 mL water) was added to the initial mixture, and the pH of the resulting solution was measured at 2.2. After 4 weeks of slow evaporation, clear plate-like crystals formed on the bottom of the vial, and yields improved upon continued crystallization for 4 additional weeks. The final product was collected via vacuum filtration, rinsed with hexanes, and allowed to dry under ambient conditions. Final yield of the product was calculated as 26.6% based upon Th.

Th_2Al_8heidi. A heterometallic solution was prepared by mixing 1.25 mL of 0.744 M $Al(NO_3)_3\cdot 9H_2O$ (0.93 mmol) and 1.25 mL of 0.211 M $Th(NO_3)_4\cdot 5H_2O$ (0.27 mmol), followed by addition of 2.5 mL of 0.248 M (0.62 mmol) of heidi. The initial pH was recorded at 1.59, and the solution was then adjusted to pH 4.23 with 230 μL of pyridine. Slow, room-temperature evaporation of the aqueous solution resulted in the formation of crystals suitable for diffraction studies after several weeks. The product was vacuum filtered and washed with hexanes, and the product yield was calculated as 12% based on Th.

Th_2Fe_2cit. Stock solutions of citric acid (0.1 M), $Fe(NO_3)_3\cdot 9H_2O$ (0.2 M), and $Th(NO_3)_4\cdot 5H_2O$ (0.2 M) were prepared in Millipure water. Solutions with 2 mL of citric acid (0.2 mmol), 2 mL of iron(III) nitrate (0.16 mmol), and 1 mL of thorium(IV) nitrate (0.11 mmol) were combined in a 20 mL glass scintillation vial and thoroughly mixed using a magnetic stir plate. The pH of the solution was increased using

DOI: 10.1021/ic502313y
Inorg. Chem. 2015, 54, 1395−1404

Table 1. Selected Crystallographic Data for $Na_4[Th_6O_2(C_{10}O_7N_2H_{14})_6]\cdot 28H_2O$ (Th_6hedta), $[Th(C_9O_6NH_{12})](NO_3)\cdot 2.5H_2O$ (Th(ntp)), $[Th_2Al_8(OH)_{14}(H_2O)_{12}(C_6O_5NH_8)_4(NO_3)_6\cdot 57H_2O$ (Th_2Al_8heidi), $[Th_2Fe_2(OH)_2(H_2O)_2(C_6O_7H_4)_2(C_6O_7H_5)_2]\cdot 5H_2O$ (ThFe(cit)), $(C_4N_2H_{12})[ThFe_2O(H_2O)_3(C_{11}O_9N_2H_{13})_2]\cdot 3.5H_2O$ ($ThFe_2$dhtpa)

	Th_6hedta	Th(ntp)	Th_2Al_8heidi	ThFe(cit)	$ThFe_2$dhtpa
space group	$P\bar{1}$	$P\bar{1}$	$P\bar{1}$	$P\bar{1}$	$P\bar{1}$
FW	3657.59	543.26	1856.46	841.19	2398.93
a (Å)	16.120(3)	8.5608(8)	15.7617(12)	9.8450(6)	10.0478(19)
b (Å)	18.483(3)	9.0331(9)	17.4826(12)	11.0807(7)	11.1790(16)
c (Å)	23.185(5)	11.1343(12)	20.0679(11)	12.7574(8)	19.543(3)
α (deg)	67.314(6)	92.821(3)	80.054(2)	67.288(2)	105.371(5)
β (deg)	87.448(6)	107.049(3)	88.890(2)	89.853(2)	90.295(6)
γ (deg)	65.143(5)	96.058(3)	67.436(2)	84.338(2)	106.281(5)
V (Å^3)	5726(2)	815.67(14)	5023.1(6)	1276.56(14)	2024.3(6)
Z	2	2	2	2	1
ρ_{calc} (mg/m^3)	2.122	2.212	1.227	2.188	1.969
μ (mm^{-1})	7.890	9.189	3.099	6.486	4.471
$F(000)$	3424	506	1776	804	1190
cryst size (mm)	0.20 × 0.18 × 0.02	0.20 × 0.15 × 0.10	0.18 × 0.05 × 0.005	0.22 × 0.20 × 0.12	0.15 × 0.09 × 0.02
θ range (deg)	2.319− 25.242	2.85−27.03	2.41−24.93	1.73−28.22	2.44−25.06
data collected	$-18 < h < 19$	$-10 < h < 10$	$-18 < h < 18$	$-13 < h < 13$	$-11 < h < 11$
	$-22 < k < 22$	$-11 < k < 11$	$-20 < k < 20$	$-14 < k < 14$	$-13 < k < 10$
	$-27 < l < 27$	$-14 < l < 14$	$-20 < l < 23$	$-16 < l < 16$	$-22 < l < 23$
reflns collected/unique	51753/20844	20229/3560	17549/14343	23811/6258	17551/6881
R_{int}	0.0506	0.0296	0.0337	0.0179	0.0720
GOF on F^2	1.053	1.073	1.069	1.129	0.987
final R indices [$I > 2\sigma(I)$]					
R_1	0.0443	0.0131	0.0305	0.0214	0.0503
R_{w2}	0.1143	0.0371	0.0378	0.0577	0.0976
R indices (all data)					
R_1	0.0607	0.0142	0.0983	0.0223	0.0896
R_{w2}	0.1241	0.0377	0.1040	0.0582	0.1134

Table 2. Summarized Data from the Thermogravimetric Analysis of $Na_4[Th_6O_2(C_{10}O_7N_2H_{14})_6]\cdot 28H_2O$ (Th_6hedta), $[Th(C_9O_6NH_{12})](NO_3)\cdot 2.5H_2O$ (Th(ntp)), $[Th_2Al_8(OH)_{14}(H_2O)_{12}(C_6O_5NH_8)_4(NO_3)_6\cdot 57H_2O$ (Th_2Al_8heidi), $(C_4N_2H_{12})[ThFe_2O(H_2O)_3(C_{11}O_9N_2H_{13})_2]\cdot 3.5H_2O$ ($ThFe_2$dhtpa)

compd	dehydration temp (°C)	wt loss (%)	calcd mol of H_2O	decompn temp (°C)	residual wt (%)	expected wt (%) (product)
Th_6hedta	100	11.7	20.6	310	49.5	48.3 (am $ThO_2\cdot Na_2O$)
Th(ntp)	125	4.6	1.38	250, 380	44.6	46.7 (ThO_2)
Th_2Al_8heidi	120	14.3	17.5	290	43.7	43.0 (2 $ThO_2\cdot 8AlOOH$)
$ThFe_2$dhpta	80	10.1	6.75	260	41.1	35.8 ($ThO_2\cdot Fe_2O_3$)

piperazine until condensation of the hydrolysis products resulted in a translucent solution. This solid phase was re-dissolved using 1 M HNO_3, resulting in a final pH of 2.35. A 1 mL aliquot of the solution was transferred into a smaller glass vial and layered with toluene in a 1:2 (vol:vol) ratio. Small brown crystals formed on the bottom of the vial after 2 months in extremely low (<2%) yields. Further attempts to improve yields in subsequent syntheses were unsuccessful.

$ThFe_2$dhpta. An aqueous solution containing 2 mL of 0.2 M $Fe(NO_3)_3\cdot 9H_2O$ (0.40 mmol) and 1 mL of 0.2 M $Th(NO_3)_4\cdot 5H_2O$ (0.20 mmol) were combined in a 20 mL glass scintillation vial. The dhpta ligand (0.065 g, 0.20 mmol) was dissolved in a separate 2 mL aliquot of water and subsequently added to the iron(III)/aluminum-(III) nitrate solution. After thorough mixing, the pH of the solution was then adjusted to 5.21 with a 1:1 mixture of pyridine and piperazine. Liquid/liquid diffusion with acetonitrile in a 1:2 ratio resulted in the formation of dark red, plate-like crystals in yields of 10% based upon Th.

X-ray Crystallography. Select crystals of each compound were isolated from the mother liquor, coated in oil to prevent dehydration during data acquisition, and mounted on a Nonius Kappa CCD single-crystal X-ray diffractometer equipped with Mo Kα radiation (λ = 0.7107 Å) and a low-temperature cryostat. Data acquisition was performed at 210 K for the samples Th(ntp), $ThFe_2$dhtpa, and Th_2Al_8heidi, while data for Th_6hedta and Th_2Fe_2cit were collected at 100 K using the Collect software.[51] Unit cell determination, data integration, and corrections for Lorentzian polarization parameters were completed using the APEX II suite of software.[52] Absorption corrections were applied using the SADABS program with the APEX II software.[52] Selected data collection parameters and crystallographic information are provided in Table 1.

Each crystal structure was initially solved by direct methods and refined on the basis of F^2 for all unique data using the Bruker SHELXTL Version 5.01 software. All five compounds were solved in the triclinic $P\bar{1}$ space group. The Th, Al, and Fe atoms were determined using direct methods solutions, and the O, C, N, and Na atoms were identified in the difference Fourier maps calculated following refinement of the partial models. Hydrogen atoms associated with the organic components were constrained using a riding model. Interstitial water molecules and charge-balancing ions were located for Th_6hedta, Th_2Fe_2cit, and $ThFe_2$dhtpa. H atoms associated with the solvent molecules were determined from the difference Fourier map following subsequent least-squares refinement of the partial structure models for $ThFe_2$dhtpa. Slight positional disorder of the water molecules in Th_6hedta and Th_2Fe_2cit did not permit location and placement of the H atoms. Significant disorder of the interstitial water was observed for Th_2Al_8heidi and Th(ntp). The diffuse electron

DOI: 10.1021/ic502313y
Inorg. Chem. 2015, 54, 1395−1404

density for both of these crystals was modeled using the SQUEEZE command in the PLATON software.[53] Crystallographic information files and tables with selected bond lengths for all five compounds are available in the Supporting Information.

Chemical Characterization. Low yields associated with Th_2Fe_2cit prohibited additional chemical characterization, but the other four compounds were further characterized by vibrational spectroscopy and thermogravimetric analysis. Purities of the bulk products were confirmed using a Bruker Advance powder diffractometer equipped with Cu Kα radiation (λ = 1.5418 Å) and a LynxEye solid-state detector. An infrared spectrum for each compound was collected from 400 to 4000 cm^{-1} using KBr as a binder on a Nicolet FTIR spectrometer. Total water content and decomposition temperatures were determined using a TA Instruments TGA Q500. Approximately 10−20 mg of each sample was loaded into an aluminum pan and heated in air from 25 to 600 °C at a ramp rate of 2 °C/min. The thermogravimetric analysis (TGA) data are summarized in Table 2, and the full weight loss curves are available in the Supporting Information.

RESULTS

Structural Descriptions. *Th_6hedta.* Two trimeric Th(IV) cores are linked via the hedta ligand to form a larger hexameric molecular species observed in the Th_6hedta compound (Figure 1). Each of the Th(IV) cations present in the core is coordinated by seven O and two N to form an overall distorted monocapped square antiprismatic coordination geometry about the metal center. Th−O bonds range from 2.322(7) to 2.516(8) Å, and slightly longer distances are observed for Th−N, with an average value of 2.784(7) Å. Overall, the hedta molecule chelates the Th(IV) cation in a hexadentate manner through the two central amines, three carboxylate functional groups, and the bridging alcohol. A trimeric unit forms through one central μ_3-O atom that is shared between three Th(IV) cations and three additional μ_2-O bridges that occur via the deprotonated alcohol groups of the hedta ligands (Figure 1a). Chelation by the hedta molecule prevents additional condensation of the metal center, but free O atoms of the carboxylate groups further coordinate to the Th(IV) cations of the neighboring trimeric unit, resulting in the formation of the final hexameric species (Figure 1b). Two crystallographically unique molecular units are observed in the lattice, although the observed bonding and coordination of the atoms in each cluster are identical. Overall, the isolated polynuclear species is approximately 14 Å in length and the molecular formula is $[Th_6O_2(hedta)_6]^{4-}$.

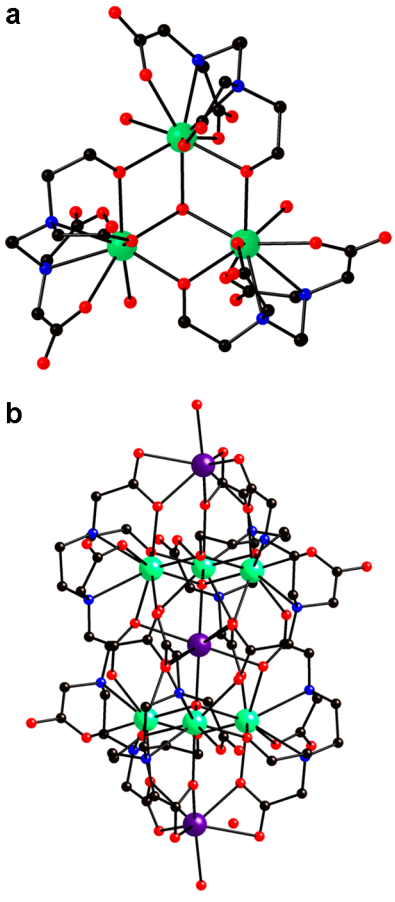

Figure 1. (a) Three Th cations bridged through a μ_3-O atom to form a trimeric group that is chelated by hedta in Th_6hedta. (b) Additional linkage between the carboxylate functional groups of the hedta ligand, converting the trimeric species into a hexameric form. Three sodium cations further coordinate to the molecule either on the interior or exterior of the cluster. Th, Na, O, C, and N atoms are represented by the green, purple, red, black, and blue spheres, respectively.

Five unique Na^+ cations are present in the solid-state structure to balance the negative charge of the cluster, and four of the five cations are closely associated with the molecular Th(IV) hexamer. One cation (Na(1) or Na(5) depending on the position of the cluster within the crystalline lattice) is located on the interior of the cluster, and two additional cations (Na(2) or Na(4)) cap the top and bottom of the trimeric units (Figure 1b). Due to steric constraints within the clusters, Na(1) and Na(5) are coordinated by eight O atoms (three carboxylate groups of the hedta ligand and the two μ_3-O atoms) with bond distances ranging from 2.412(10) to 2.627(9) Å. Na(2) and Na(4) are coordinated by six O atoms associated with the three carboxylate functional groups and an additional water molecule. Distances between the cation and the H_2O molecule are observed at 2.412(10) or 2.466(11) Å for Na(2)−O(33) and Na(4)−O(39), respectively. Slightly longer bond distances are found between the Na cations and the carboxylate O atoms (2.442(10) to 2.627(9) Å).

Additional coordination with a third distinct Na cation (Na(3)) and supramolecular interactions with the solvent water molecules lead to the crystallization of the hexameric Th(IV) molecules into a solid-state compound. Na(3) is positioned between the hexameric clusters and possesses a distorted octahedral geometry with bond distances ranging between 2.306(10) and 2.876 (16) Å (Supporting Information Figure S3). One water molecule (O33) interacts with both Na(2) and Na(3) to link the individual atoms into a sodium tetramer, which further connects one of the crystallographically unique hexamers to its neighbor and forms an extended one-dimensional (1-D) chain structure. The second unique hexameric unit and additional water molecules are also located between the chains, linking them into the 3-D crystalline lattice through hydrogen bonding interactions. The presence of Na cations and water molecules in the interstitial regions results in a solid-state compound with the overall formula of $Na_4[Th_6O_2(hedta)_6]\cdot 28H_2O$.

Th(ntp). Unlike the Th_6hedta compound, condensation of Th(IV) is prevented by the presence of the organic chelator, but the ntp ligand enables linkages between the individual metal centers that result in an extended topology. Each Th(IV) cation is coordinated by nine O atoms to form a distorted monocapped square antiprism with bond lengths ranging from

DOI: 10.1021/ic502313y
Inorg. Chem. 2015, 54, 1395−1404

2.337(5) to 2.592 Å (Figure 2a). One nitrate anion in bidentate coordination occupies two of the binding sites, six O atoms are associated with the ntp ligand, and the coordination sphere is completed by one additional water molecule. The central amine group remains uncomplexed by the metal center, and each Th(IV) polyhedra is linked through the free ntp carboxylate group to form the extended 2-D sheet topology (Figure 2b). It is important to note that Al(III) is also present in this synthesis, but a heterometallic species does not form under these conditions. Additional water groups are located in the interstitial region, linking the 2-D sheets into the crystalline lattice through hydrogen bonding interactions and forming a solid-state material with an overall formula of $[Th(C_9O_6NH_{12})(H_2O)(NO_3)]\cdot 2.5H_2O$.

Th_2Al_8heidi. The ternary molecular species observed in Th_2Al_8heidi is based upon a hexameric Al(III) core that is created through condensation of the metal cations (Figure 3). Each of the Al(III) atoms in the central unit are coordinated to six OH or H_2O groups to form an octahedral coordination geometry, with bond distances ranging from 1.827(3) to 1.988(3) Å. Four of the Al atoms are linked through bridging hydroxyl groups and create the $Al_4(\mu_2\text{-}OH)_{14}(H_2O)_2$ cubane-like unit. Two additional Al(III) octahedra bind in a bridging bidentate fashion to the top and bottom of the tetramer to form the hexameric core.

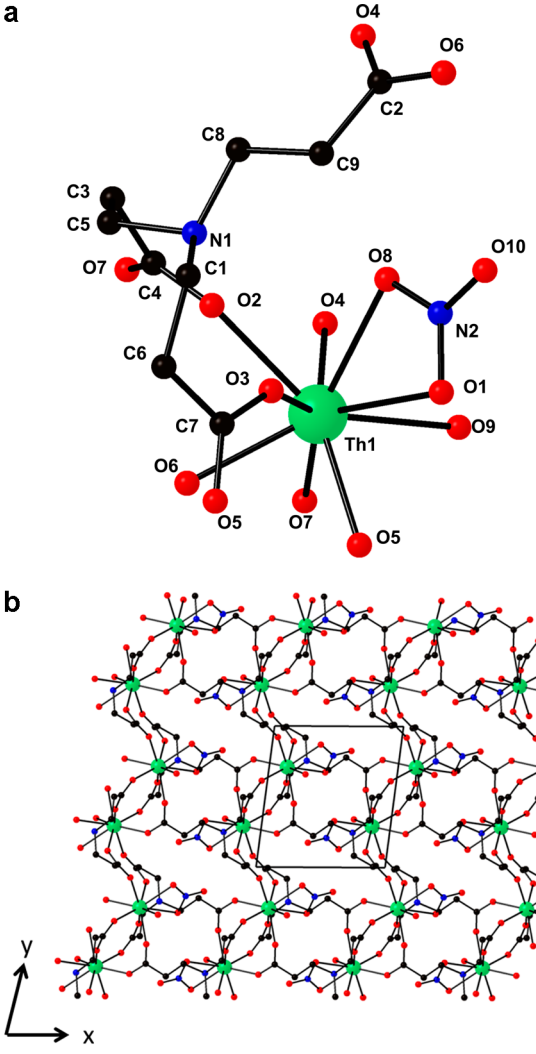

Figure 2. (a) One ntp ligand and one nitrate anion bonding to the Th(IV) cation in a bidentate manner to create the fundamental building unit of Th(ntp). (b) ntp molecule further linking the Th(IV) cation into a 2D sheet through the free deprotonated carboxylate functional group. Th, O, C, and N atoms are represented by the green, red, black, and blue spheres, respectively.

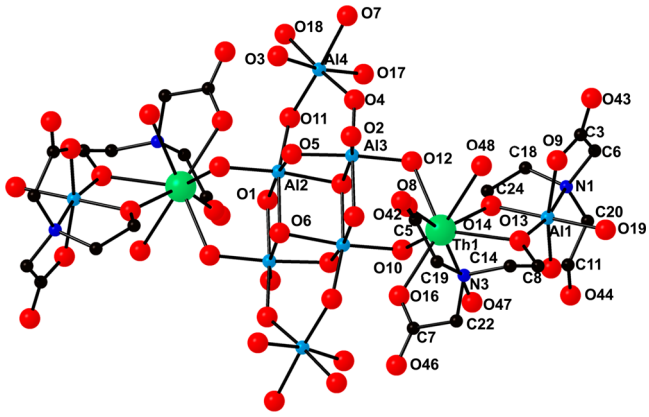

Figure 3. Eight Al atoms (turquoise spheres) forming the central core of the cluster observed in Th_2Al_8heidi. Two heterometallic Th/Al dimers chelated by the heidi ligands bond to either side of the molecular unit to form $[Th_2Al_8(OH)_{14}(H_2O)_{12}(C_6O_5NH_8)_4]^{6+}$.

Two mixed-metal Al(III)/Th(III) dimers are formed through chelation with the heidi molecule and bond to the exterior of the hexameric Al(III) core. For each dimer, two ligands chelate the Th(IV) and Al(III) cations in a tetradentate manner through the carboxylate, hydroxyl, and amine functional groups. Additional water groups are bonded to the Al(III) and Th(IV) cations to complete the octahedral and distorted monocapped square antiprismatic coordination spheres, respectively. Th−O bond distances range from 2.383(3) to 2.640(3) Å, and, as expected, the Th−N distances are elongated by approximately 0.1 Å. The metal centers are bridged through the deprotonated alcohol group, and the Th(IV) component of the dimer link to the central Al(III) core in a bridging bidentate fashion. The overall cluster is positively charged and has a molecular formula of $[Th_2Al_8(OH)_{14}(H_2O)_{12}(C_6O_5NH_8)_4]^{6+}$.

These ternary species are arranged into a porous 2-D structure through supramolecular interactions with neighboring clusters. H atoms associated with the central core interact with the heidi ligands on the adjacent molecules to create 2-D layers that are 12 Å in width. Within the layers, elongated pores spaces that are 6 × 10 Å in diameter house additional charge-balancing nitrate anions and neutral water molecules to form the compound $[Th_2Al_8(OH)_{14}(H_2O)_{12}(C_6O_5NH_8)_4](NO_3)_6\cdot 57H_2O$.

Th_2Fe_2cit. A tetrameric molecular species is the central structural feature of the Th_2Fe_2cit compound (Figure 4a). Each Fe(III) cation is coordinated by six ligands with an average Fe−O bond length of 2.011(2) Å. The two Fe(III) atoms are bridged through two central O atoms, which are also coordinated to an additional Th(IV) cation to form μ_3-O bridges within the tetrameric core. Four cit molecules are located on the exterior of the metal core, and the deprotonated alcohol groups of the ligand create additional bridging groups between the Fe(III) and Th(IV) cations. Chelation by the cit ligand completes the octahedral geometry about the Fe(III) cations, but the ligand plus an additional water molecule is necessary to complete the Th(IV) coordination shell. Addition

DOI: 10.1021/ic502313y
Inorg. Chem. 2015, 54, 1395−1404

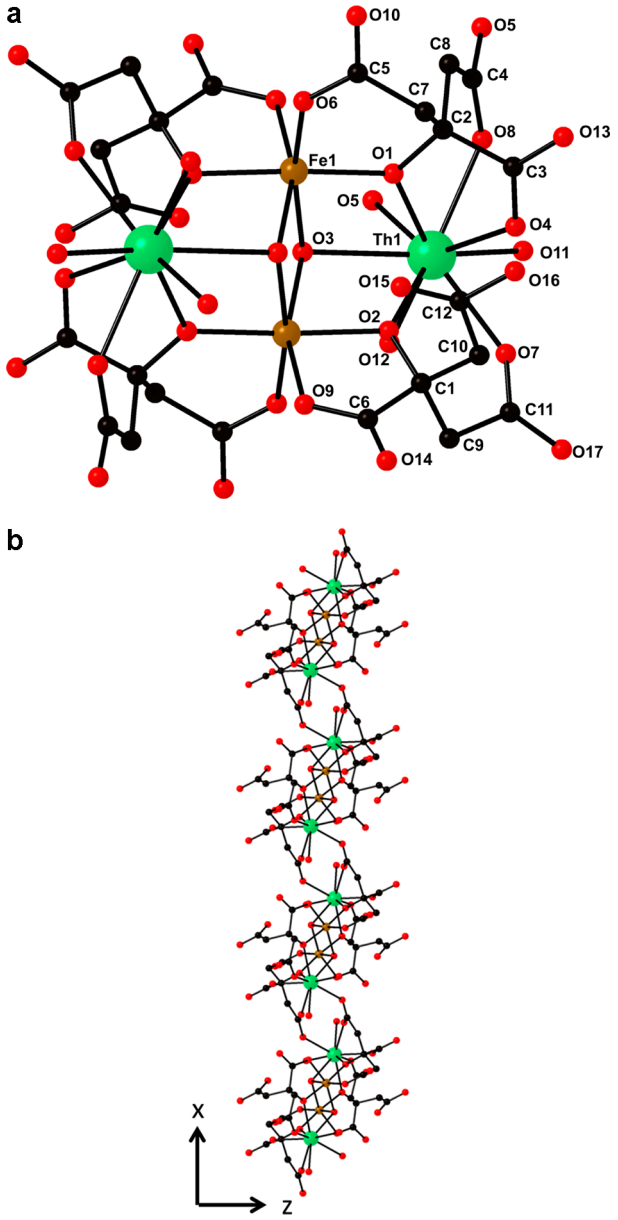

Figure 4. (a) Th_2Fe_2cit containing a tetrameric species with two Fe(III) (brown spheres) and two Th(IV) cations, bridged through two μ_2-OH groups and chelated by cit molecules. (b) Carboxylates associated with the cit ligand linking the individual molecular species into a 1D chain topology.

of the aqua ligand results in a coordination number of nine and Th−O bond lengths that range from 2.387(3) to 2.563(2) Å. While two cit molecules are observed in tetradentate coordination to the Fe(III) and Th(IV) cations, the other two cit contain one protonated, noncomplexed carboxylate arm ($[Th_2Fe_2(OH)_2(H_2O)_2(C_6O_7H_4)_2(C_6O_7H_5)_2]^{2-}$).

The presence of a free carboxylate group should promote the formation of an extended structure, but the tetrameric clusters are instead linked into a 1-D chain through the complexed arms of the cit ligand (Figure 4b). More specifically, the O atoms associated with the carboxylate functional groups further link the molecular core into an extended array and each of the free carboxylate arms extend from either side of the chains. These protonated arms are available for additional H bonding interactions with the piperazinium cations and the interstitial water molecules, leading to the crystallization of the solid-state material. With the presence of charge-balancing cations and solvent, the overall formula for the Th_2Fe_2cit compound is $(C_4N_2H_{12})[Th_2Fe_2(OH)_2(H_2O)_2(C_6O_7H_4)_2(C_6O_7H_5)_2]\cdot 5H_2O$.

$ThFe_2dhpta$. Two dhpta ligands chelate the Th(IV) and Fe(III) cations to form the isolated molecular species observed in $ThFe_2dhpta$ (Figure 5). Each of the Fe(III) cations are complexed to six ligands, forming a distorted octahedral coordination geometry with average Fe−O and Fe−N bond lengths of 1.981(6) and 2.260(7), respectively. The Th(IV) cation is coordinated to eight O atoms and two N atoms for a total coordination number of 10 and molecular geometry that can be described as a bicapped square antiprism. Both dhpta ligands completely chelate the central $ThFe_2$ unit and bridge the metal centers through the deprotonated alcohol group. An additional μ_3-O bridge occurs through the O(5) atom, with the remainder of the inner-sphere coordination sites occupied by water molecules. Overall the molecule is neutral, with interstitial water molecules participating the hydrogen bonding interactions to create the solid $[ThFe_2O(H_2O)_3(C_{11}O_9N_2H_{13})_2]\cdot 3.5H_2O$ compound.

Infrared Spectroscopy. The infrared spectra of the binary and ternary Th(IV) compounds contain features that are characteristic of the presence of molecular water and the polycarboxylate ligands (Figure 6). Stretching vibrations for the O−H bonds are observed between 2700 and 3600 cm^{-1}, corresponding to the complexed and free solvent water molecules that are present in each of the compounds. The bending mode for the solvent water molecules also appears at approximately 1640 cm^{-1} and is observed for all of the hydrated compounds. A strong band located near 1400 cm^{-1} has been identified as the carboxylate groups associated with the organic ligands that are complexed to the Al(III), Fe(III), or Th(IV) metal centers. Protonated carboxylate groups have vibrational modes at approximately 1700 cm^{-1} and are noticeably absent, confirming the deprotonation and complexation of all carboxylate groups. Nitrate anions are present in Th(ntp) and Th_2Al_8heidi, and the N−O antisymmetric stretching vibration is expected at approximately 1350 cm^{-1}; however, overlap with stronger bands associated with the deprotonated

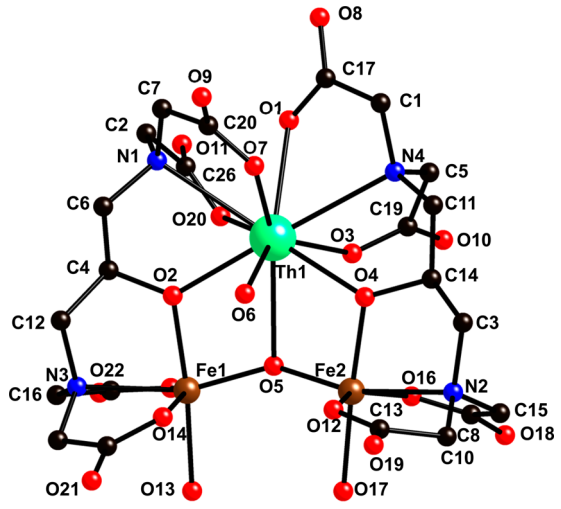

Figure 5. Two Fe(III) atoms (brown spheres) and one Th(IV) atom forming the core molecular unit in $ThFe_2dhpta$, with two dhpta molecules chelating the trimeric species.

DOI: 10.1021/ic502313y
Inorg. Chem. 2015, 54, 1395−1404

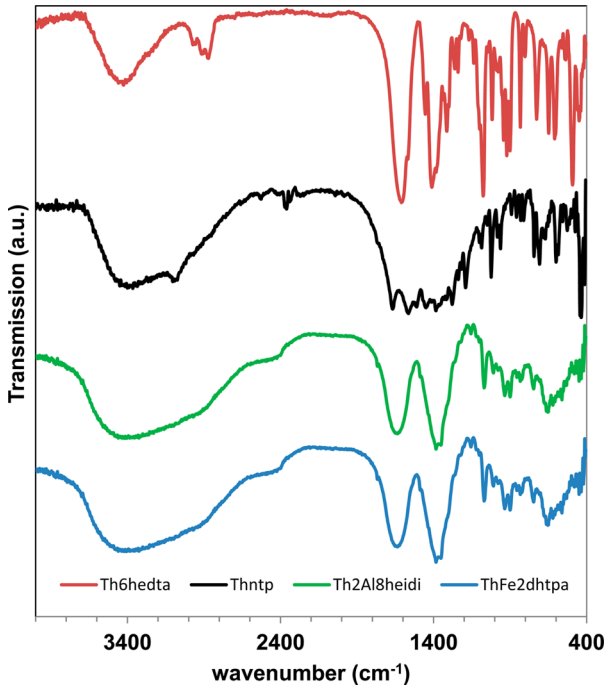

Figure 6. Infrared spectroscopy of the binary and ternary Th(IV) complexes.

carboxylate groups leads to difficulties in specifically determining these modes. Weaker vibrational modes at lower wavenumbers in all spectra are associated with C−H, N−C, and C−C modes associated with the aliphatic backbone of the carboxylate ligand.

Thermogravimetric Analysis. Initial weight loss of the binary and ternary Th(IV) compounds occurs between 80 and 125 °C, corresponding to the removal of weakly bound water molecules located in the interstitial regions of the crystalline lattice. The experimental mass loss associated with dehydration of the sample as determined by TGA were compared to the predicted values from single-crystal X-ray diffraction data and were found to contain some variability (Table 2). These differences are likely caused by the significant amounts of loosely bound interstitial water molecules, and dehydration of the material is unavoidable during the filtration process. Within the temperature regime associated with removal of interstitial water molecules, a secondary weight loss of 7.1% was observed for $ThFe_2$dhpta compound that was related to the removal of the piperazinium cation (7.7% expected). Second major mass losses in the TGA data are linked to the degradation of the polycarboxylate ligands, which occurs between 250 and 380 °C. Additional structural water molecules are lost within this region for the Th_2Al_8heidi compound as seen by a gradual decrease in the overall sample mass. The final products in all samples were determined to be amorphous by powder X-ray diffraction, with residual weights between 38.6 and 49.5%. For Th(ntp), the final product is expected to be amorphous ThO_2 and Th_6hedta forms a composite material containing a mixture of amorphous ThO_2 and Na_2O solids. For each of the ternary complexes, the residual weights also suggested a mixture of solid-state thorium(IV)/iron(III), aluminum(III) oxide materials. Powder X-ray diffraction of the $ThFe_2$dhpta solid after TGA indicated the formation of crystalline ThO_2 and Fe_2O_3, but due to the larger residual weights observed for this sample, amorphous material is also likely in the residual product.

DISCUSSION

Th^{4+} Hydrolysis. Hydrolysis and condensation of the Th(IV) cation occurs quite readily when the pH of the solution is >2 and the metal concentration is >0.1 mM.[4] The condensation reaction can occur either as olation, by the removal of a single proton from a H_2O molecule to form a hydroxyl bridge, or as oxolation, which occurs when water is released as a leaving group and an O atom is shared between two or more metal centers.[3,6] While the different pathways create different ligand bridges, both result in the formation of polynuclear species that can range from small dimeric units to nanoscale molecular clusters.[1,2,4] In aqueous solutions, monomers ($Th(OH)_3^+$ and $Th(OH)_2^{2+}$), dimers ($Th_2(OH)_2^{6+}$), tetramers ($Th_4(OH)_{12}^{4+}$), and hexamers have previously been identified as the dominant species through potentiometric means.[4]

The presence of an organic chelator in solution during the hydrolysis reaction can have significant impacts on the resulting species. Excellent examples of this phenomenon were reported by Hu et al.,[34] and Takao et al.,[54] in which high-energy X-ray scattering (HEXS) or EXAFS was utilized to monitor the impact of the Th(IV) hydrolysis of when glycine, or formate, was added to the system. In the absence of the carboxylate ligand, μ_2-OH bridged dimeric species were dominant and remained stable for an extended time period.[34] Upon addition of the organic ligand, the dimeric species condensed to form a $[Th_6(\mu_3\text{-}O)_4(\mu_3\text{-}OH)_4]^{12+}$ hexameric cluster chelated by 12 glycine or formate molecules.[34,54] The same hexameric cluster has been synthesized by the dissolution of amorphous Th(IV) oxide/hydroxide solids with formic, acetic, and chloroacetic acids, suggesting that the overall presence of small carboxylate containing ligands may promote the formation of this specific species.[27,54] The hedta ligand contains multiple carboxylate groups, and the size and ability to chelate in a tetradentate fashion seem to favor the trimeric species, although formation the hexameric cluster still occurs through the organic molecule.

In addition to the complexing ligands, the presence and close association of the Na cations may also influence the overall condensation product. Three of the Na cations are closely associated with Th(IV) hexamer, as they are directly linked to the hedta ligand and are located 4.56−4.62 Å from the metal cations within the cluster. This includes the Na atoms on the top and bottom of the clusters, which are essentially free to position themselves anywhere within the crystalline lattice. The cavity created by the carboxylate functional group, both inside and outside the cluster, seems to be ideal for the placement of the Na cation and may further impact the structural nature of the hydrolysis product. The importance of counterions in the formation of condensation products has also been observed in other systems, most notably through the role of sulfate in Zr(IV) hydrolysis. Hu et al.[55] have combined solution-based HEXS studies with solid-state structural characterization to demonstrate that increased sulfate concentrations that resulted in the formation of larger condensation products via bridging sulfate anions. Additional work on niobium polyoxometalates indicated that the extent of oligomerization was controlled by the identity of the charge-balancing cation.[5]

Th^{4+}/Al^{3+} Hydrolysis. To form ternary hydrolysis products, the solution conditions must promote the deprotonation of the aqua complexes of both metal species or prevent the formation of binary species. The Th(ntp) compound demonstrates this principle because Al(III) and Th(IV) cations are present in

DOI: 10.1021/ic502313y
Inorg. Chem. 2015, 54, 1395−1404

solution, but condensation of either metal is prevented through a combination of the low solution pH and chelation by the organic ligand. Hydrolysis of the Th(IV) cation begins at a pH of 1.5−2.5, whereas the pH must be closer to 3.0 to favor the formation of Al(III) dimers.[1,3,56] Synthetic conditions for the Th(IV) monomer are favored in this case because pH of the solution is 2.2, and this also precludes the hydrolysis and condensation of the Al(III). Therefore, ternary structures are not likely to form in these conditions. Presence of the ntp ligand also plays a role by chelating the Th(IV) metal center and further preventing the formation of the polynuclear species through additional condensation reactions. The large coordination shell of the Th(IV) cation inhibits the ntp molecule from encapsulating the metal center, but the free carboxylate groups on the neighboring molecule can bind to create a 2-D sheet.

Condensation of the Th(IV) cation can also be thwarted by the presence of other polycarboxylate molecules, and topological differences of the resulting extended structures are based upon the identity of the chelators. A related ligand, nitrilotriacetic acid, forms a Th(IV) sheet topology through a combination of chelation of the metal center and linkage through the protonated forms of the molecule.[57] Presence of other polycarboxylates, such as iminodiacetate, ethylenediaminetetracetate, and several forms of pyridinedicarboxylate ligands, all create extended topologies with different structural features based upon the chelation mode of the ligands.[57,58] All of the previously reported compounds were formed at low pH values, suggesting that hydrolysis was not the dominate chemical process and that the ligand coordination is the major driver in the formation of extended structures.

Increasing the pH of the solution promotes the hydrolysis of both the Al(III) and Th(IV) cations and subsequent condensation reactions to form larger oligomers. Solid-state and aqueous experiments indicate that olation is the predominate mechanism for the aquahydroxo complexes of Al(III), resulting in the isolation of "flat" molecular species, such as $[Al_{13}(\mu_3\text{-}OH)_5(\mu_2\text{-}OH)_{18}(H_2O)_{24}]^{15+}$.[59,60] Oxolation can also be observed for Al(III) polynuclear clusters when the hydrolysis rate is increased, favoring the formation of the AlO_4 tetrahedron that occupies the central core of the Keggin-type species.[1,60] Structural characterization of solid-state thorium compounds suggests that condensation of the Th(IV) cation can also take place through either mechanism with hydroxyl bridges predominant among smaller dimers and mixed oxo/hydroxo bridges observed in larger oligomers. Under slightly acidic to neutral conditions, chelation by organic molecules can still occur, but does not significantly inhibit the hydrolysis or condensation reactions, as demonstrated by the formation of the $[Al_{13}(\mu_3\text{-}OH)_6(\mu_2\text{-}OH)_{12}(heidi)_6(H_2O)_6]^{3+}$ and $[Al_{15}(\mu_2\text{-}O)_4(\mu_3\text{-}OH)_6(\mu_2\text{-}OH)_{14}(hpdta)_4]^{3-}$ clusters.[18,61]

The formation of heterometallic polynuclear species may be driven by similarities in the condensation mechanism, but structural topologies are likely influenced by the presence of the organic chelator. Bond valence calculations of the shared O atoms associated with the molecular species in Th_2Al_8heidi suggest that they are indeed hydroxyl groups and that olation is the likely pathway. Similarities between condensation mechanisms may lead to more interactions in solution and the formation of heterometallic species upon hydrolysis. Several heterometallic Al(III)/Th(IV) polynuclear species have been previously identified and some topological differences can be determined based upon the size of the chelating ligand. The cubane-like $[Al_4(\mu_2\text{-}OH)_{14}(H_2O)]$ moiety is a dominate feature in these clusters forming the core of the $[Th_2Al_6(OH)_{14}(H_2O)_{12}(hedta)_2]^{6+}$, $[Th_2(H_2O)_2Al_6(H_2O)_{10}(OH)_{14}(edta)_2]^{4+}$, and $[Th_4(H_2O)_4Al_{10}(H_2O)_8(OH)_{28}(edta)_4]^{2+}$ complexes.[49,50] For these heterometallic species, the organic chelating ligands are only complexed to the Th(IV) cations and thus do not impact the structural characteristics of the of the Al(III) core. When the organic ligand becomes larger, then heterometallic dimeric units can occur and alter the structural nature of the resulting condensation product. In the case of the previously reported $[Th_2Al_8(OH)_{12}(H_2O)_{10}(dhpta)_4]$ species, the molecular species contains three distinct dimeric building blocks: (1) an uncomplexed $Al_2(OH)_8$ unit; (2) two complexed $Al_2(dhpta)(H_2O)_2$ species; and (3) two heterometallic ThAl(dhpta)$(H_2O)_3$ components.[49] It is important to note that all of these compounds have been identified in the solid state and very little information is available regarding heterometallic Al(III)/Th(IV) species that exist in aqueous solutions.

Th(IV)/Fe(III) Hydrolysis. Structural characterization of Fe(III) polynuclear clusters can be found in the literature, but Th(IV)/Fe(III) species have not been previously reported. A majority of the characterized clusters are comprised of octahedrally coordinated Fe(III) cations arranged in a "flat" configuration and chelated by polyaminocarboxylate ligands.[62−65] An iron(III) citrate compound containing a trimeric Fe(III) core has also been observed that contains three μ_2-OH bridges and a central μ_3-O group.[66] This complex is similar to the Th_2Fe_2cit compound because additional linkages occur between the trimeric species to form an extended species; however, the 1-D chain in the binary form is terminated, forming a nonairon(III) citrate complex.

While little is known about aqueous systems containing both Th(IV) and Al(III), heterometallic Th(IV)/Fe(III) solutions have been the subject of several studies. For example, Davydov and Toropov[39] observed increased solubility of the mixed-metal system compared to the related single phases and suggested the formation of polynuclear species in solution. Torapova et al.[67] corroborated these results with EXAFS spectroscopy and large-angle X-ray scattering (LAXS) studies, which identified a Th_2Fe_2 tetrameric species in solution. Additional potentiometric titrations suggested the formation of polynuclear species with the proposed composition of $[Th_2Fe_2(OH)_8(H_2O)_{12}]^{6+}$, and ultrafiltration and X-ray scattering studies indicate that the overall diameter of the cluster is approximately 16 Å.

Structural information provided in the EXAFS studies suggests the formation of a different species present in the prepared solutions, compared to the molecular species present in Th_2Fe_2cit or $ThFe_2$dhpta.[67] The Fe−Fe distances obtained from the EXAFS studies on two different solutions were 3.044(8) and 3.035(3) Å, which are slightly shorter than the interatomic distance observed in Th_2Fe_2cit (3.169(1) Å) and deviate significantly from those in $ThFe_2$dhpta (3.496(6) Å). The Th−Th interatomic distances were also reported at 3.938(1) and 3.941(1) Å, respectively, and again, these values are much shorter than the distance of 6.626(1) Å observed in Th_2Fe_2cit.[67] The absence of organic chelators in the previous studies may play a major role in explaining the structural differences, but additional studies are necessary to determine the dominant aqueous species under these conditions.

Relationships to Environmental Systems. Colloidal transport by Fe(III) and Al(III) oxyhydroxide phases has been implicated in the enhanced transport of insoluble tetravalent actinides in environmental systems, and similarities

DOI: 10.1021/ic502313y
Inorg. Chem. 2015, 54, 1395−1404

in metal hydrolysis and condensation mechanisms may play a key role in the binding affinities. Stumm et al.[68] first noted that the ability of a metal cation to bind to surface hydroxyl groups is related to the propensity to form hydrolysis complexes in solution. This relationship was also highlighted by Whitfield and Turner,[69] who created a complex field diagram for scavenging of trace metals in seawater. Hydrolytic scavenging in seawater corresponded to strongly hydrolyzed elements (Al(III), Cr(III), Fe(III), Ga(III), Hf(IV), Th(IV), U(IV), and Zr(IV)). This relationship suggested that particle reactivity or colloidal adsorptivity in marine environments can be linked to the similarities in metal hydrolysis and condensation reactions.

Interactions of Th(IV) with the mineral surfaces have been previously explored with a range of chemical characterization techniques, and high adsorption capabilities have been linked to inner-sphere coordination sites and the presence of oligomeric species. Osthols[70] utilized radiometric measurements and EXAFS spectroscopy to determine that Th(VI) binds through an inner-sphere coordination mechanism on the surface of amorphous silica. Degueldre and Kline[71] investigated several mineral surfaces using geochemical models and observed that the strength of Th(IV) adsorption increases through the series $SiO_2 < Fe_2O_3 < Al_2O_3 < TiO_2$, which may be related to the number of oxo or hydroxo sites available for binding. In the same study, oligomers were postulated to exist on the mineral surface when Th(IV) concentrations were greater than 10^{-3} M, and the authors suggested that these units were initially formed in solution before adsorption to the mineral surface occurred.[71] Polynuclear species were then observed experimentally on the aluminosilicates mineral, muscovite, using crystal truncation rod and resonant anomalous X-ray reflectivity measurements, but only when concentrations were greater than 2.0×10^{-3} M.[72]

The exact nature of the adsorption of Th(IV) on the surface of iron(III) and aluminum(III) oxyhydroxide colloids has not been determined, but studies investigating mineral surfaces can be found in the literature. Seco et al.[73] investigated the adsorption of Th(IV) onto steel corrosion products (two-line ferrihydrite and magnetite) by EXAFS spectroscopy and found that, in both phases, the Th(IV) complexed to the iron oxide surface through oxo bridges. In the case of ferrihydrite, two O subshells were observed, one at 2.37 Å that was associated with the bridging surface groups and another at 2.54 Å for the nonbridging water molecules located in the first-coordination sphere. Th−Fe distances were observed at approximately 3.60 Å, and Seco et al.[73] suggested that the Th−Fe distances were the result of a bridging bidentate coordination with two Fe(III) octahedra located on the ferrihydrite surface. Th(IV) adsorbed to the magnetite surface through oxo bridges with bond lengths of 2.40 Å and two distinct Th−Fe distances at 3.51 and 3.69 Å. Structural models of the data suggest that the Th(IV) adsorbs to the magnetite surface as a bridging bidentate coordination between both Fe(III) octahedra and tetrahedra.

The Th−Fe distances reported by Seco et al.[73] agree well with the models provided by Th_2Fe_2cit and $ThFe_2$dhpta where the Th(IV) cation bridges two Fe(III) metal centers. Interestingly, both molecules also contain a third bond (the μ_3-O group) between the Th(IV) and Fe(III) centers, which is slightly elongated at 2.563(2) and 2.617(5) Å. Therefore, variation in the O subshell for the ferrihydrite sample could also be interpreted as an additional bond to the mineral surface, or at least masked by the presence of additional water molecules in the first-coordination shell. Agreement between the EXAFS data provided by Seco et al.[73] demonstrates the importance of these molecular models for interpreting real-world, environmental samples.

CONCLUSION

The current study provided the synthesis and characterization of five Th(IV) and mixed Th(IV)/(Fe(III),Al(III)) compounds. These binary and ternary Th(IV) complexes provide additional molecular-level details on the subtle interplay of chelation and condensation within these systems. While differences were observed between previously reported solution-based studies and the model compounds, the isolated complexes provide insight into adsorption onto mineral surfaces. Continued efforts to isolate structural models with environmental relevance and future studies relating these finding to aqueous solutions will provide additional understanding and insight into the mechanism of adsorption and transport of contaminant species in natural waters.

ASSOCIATED CONTENT

Supporting Information

Crystallographic information files (CIFs), bond distance tables, and figures showing atomic labeling, packing diagrams, and thermogravimetric analysis. This material is available free of charge via the Internet at http://pubs.acs.org.

AUTHOR INFORMATION

Corresponding Author

*E-mail: tori-forbes@uiowa.edu.

Notes

The authors declare no competing financial interest.

ACKNOWLEDGMENTS

We acknowledge the University of Iowa College of Liberal Arts and Sciences, Vice President for Research Math and Physical Sciences Funding Program, and Center for Global and Environmental Research for providing support for the mixed-metal hydrolysis projects. We also thank Dr. Edward Gillan for use of the FTIR spectrometer.

REFERENCES

(1) Casey, W. H. *Chem. Rev.* **2006**, *106*, 1−16.
(2) Casey, W. H.; Phillips, B. L.; Furrer, G. *Rev. Mineral. Geochem.* **2001**, *44*, 167−190.
(3) Baes, C. F.; Mesmer, R. E. *The hydrolysis of cations*; John Wiley and Sons: New York, NY, USA, 1976.
(4) Knope, K. E.; Soderholm, L. *Chem. Rev.* **2013**, *113*, 944−994.
(5) Hou, Y.; Zakharov, L. N.; Nyman, M. *J. Am. Chem. Soc.* **2013**, *135*, 16651−16657.
(6) Jolivet, J.-P.; Chaneac, C.; Chiche, D.; Cassaignon, S.; Durupthy, O.; Hernandez, J. *C. R. Geosci.* **2011**, *343*, 113−122.
(7) Furrer, G.; Phillips, B. L.; Ulrich, K. U.; Pothig, R.; Casey, W. H. *Science* **2002**, *297*, 2245−2247.
(8) Cheng, X. L.; Liu, Y. J.; Chen, D. R. *J. Phys. Chem. A* **2011**, *115*, 4719−4728.
(9) Akitt, J. W.; Elders, J. M. *J. Chem. Soc., Dalton Trans.* **1988**, *83*, 1347−1355.
(10) Akitt, J. W.; Elders, J. M. *J. Chem. Soc., Faraday Trans. 1* **1985**, *81*, 1923−1930.
(11) Heath, S. L.; Jordan, P. A.; Johnson, I. D.; Moore, G. R.; Powell, A. K.; Helliwell, M. *J. Inorg. Biochem.* **1995**, *59*, 785−794.
(12) Amini, M. M.; Sharbatdaran, M.; Mirzaee, M.; Mirzaei, P. *Polyhedron* **2006**, *25*, 3231−3237.
(13) Joszai, R.; Kerekes, I.; Satoshi, I.; Sawada, K.; Zekany, L.; Toth, I. *Dalton Trans.* **2006**, *26*, 3221−3227.

DOI: 10.1021/ic502313y
Inorg. Chem. 2015, 54, 1395−1404

(14) Abeysinghe, S.; Unruh, D. K.; Forbes, T. Z. *Cryst. Growth Des.* **2012**, *12*, 2044−2051.
(15) Sun, Z.; Wang, H.; Tong, H.; Sun, S. *Inorg. Chem.* **2011**, *50*, 559−564.
(16) Allouche, L.; Gerardin, C.; Loiseau, T.; Ferey, G.; Taulelle, F. *Angew.Chem., Int. Ed.* **2000**, *39* (3), 511−514.
(17) Johansson, G. *Acta Chem. Scand.* **1960**, *14*, 771−773.
(18) Schmitt, W.; Baissa, E.; Mandel, A.; Anson, C. E.; Powell, A. K. *Angew. Chem., Int. Ed.* **2001**, *40*, 3578−3580.
(19) Wang, W.; Wentz, K. M.; Hayes, S. E.; Johnson, D. W.; Keszler, D. A. *Inorg. Chem.* **2011**, *50*, 4683−4685.
(20) Hunter, D.; Ross, D. S. *Science* **1991**, *251*, 1056−1058.
(21) Mensinger, Z. L.; Wang, W.; Keszler, D. A.; Johnson, D. W. *Chem. Soc. Rev.* **2012**, *41*, 1019−1030.
(22) Mujika, J. I.; Ugalde, J. M.; Lopez, X. *Phys. Chem. Chem. Phys.* **2012**, *14*, 12465−12475.
(23) Schmitt, W.; Anson, C. E.; Pilawa, B.; Powell, A. K. *Z. Anorg. Allg. Chem.* **2002**, *628*, 2443−2457.
(24) Steppert, M.; Walther, C.; Fuss, M.; Buchner, S. *Rapid Commun. Mass Spectrom.* **2012**, *26*, 583−591.
(25) Gerasko, O. A.; Mainicheva, E. A.; Nauvmov, D. Yu.; Kuratieva, N. V.; Sokolov, M. N.; Fedin, V. P. *Inorg. Chem.* **2005**, *44*, 4133−4135.
(26) Knope, K. E.; Vasiliu, M.; Dixon, D. A.; Soderholm, L. *Inorg. Chem.* **2012**, *51*, 4239−4249.
(27) Knope, K. E.; Wilson, R. E.; Vasiliu, M.; Dixon, D. A.; Soderholm, L. *Inorg. Chem.* **2011**, *50*, 9696−9704.
(28) Kalaji, A.; Skanthakumar, S.; Kanatzidis, M. G.; Mitchell, J. F.; Soderholm, L. *Inorg. Chem.* **2014**, *53*, 6321−6328.
(29) Fang, Z.; Dixon, D. A. *J. Phys. Chem. C* **2013**, *117*, 7459−7474.
(30) Falaise, C.; Volkringer, C.; Vigier, J.-F.; Beaurain, A.; Roussel, P.; Rabu, P.; Loiseau, T. *J. Am. Chem. Soc.* **2013**, *135*, 15678−15681.
(31) Unruh, D. K.; Gojdas, K.; Flores, E.; Libo, A.; Forbes, T. Z. *Inorg. Chem.* **2013**, *52*, 10191−10198.
(32) Schlesinger, M.; Weber, M.; Rueffer, T.; Lang, H.; Mehring, M. *Eur. J. Inorg. Chem.* **2014**, *2014*, 302−309.
(33) Miersch, L.; Schlesinger, M.; Troff, R. W.; Schalley, C. A.; Rueffer, T.; Lang, H.; Zahn, D.; Mehring, M. *Chem.—Eur. J.* **2011**, *17*, 6985−6990.
(34) Hu, Y.-J.; Knope, K. E.; Skanthakumar, S.; Soderholm, L. *Eur. J. Inorg. Chem.* **2013**, *24*, 4159−4163.
(35) Woidy, P.; Kraus, F. *Z. Anorg. Allg. Chem.* **2014**, *640*, 1547−1550.
(36) Batuk, O. N.; Szabo, D. V.; Denecke, M. A.; Vitova, T.; Kalmykov, S. N. *Radiochim. Acta* **2013**, *101*, 233−239.
(37) Takasaki, F.; Fujiwara, K.; Nakajima, Y.; Nishikawa, T.; Ogawa, N. *Chem. Lett.* **2014**, *43*, 196−198.
(38) Mensinger, Z. L.; Gatlin, J. T.; Meyers, S. T.; Zakharov, L. N.; Keszler, D. A.; Johnson, D. W. *Angew. Chem., Int. Ed.* **2008**, *47*, 9484−9486.
(39) Davydov, Y. P.; Toropov, I. G. *Proc. Natl. Acad. Sci. Belarus, Chem. Ser.* **1986**, *5*, 7−10.
(40) Wei, Z.; Han, H.; Filatov, A. S.; Dikarev, E. V. *Chem. Sci.* **2014**, *5*, 813−818.
(41) Simond, D.; Clifford, S. E.; Vieira, A. F.; Besnard, C.; Williams, A. F. *RSC Adv.* **2014**, *4*, 16686−16693.
(42) Sato, R.; Suzuki, K.; Sugawa, M.; Mizuno, N. *Chem.—Eur. J.* **2013**, *19*, 12982−12990.
(43) Hashimoto, Y. *Appl. Geochem.* **2007**, *22*, 2861−2871.
(44) Pasilis, S. P.; Pemberton, J. E. *Inorg. Chem.* **2003**, *42*, 6793−6800.
(45) Dodge, C. J.; Francis, A. J. *Radiochim. Acta* **2003**, *91*, 525−532.
(46) Dodge, C. J.; Francis, A. J. *Environ. Sci. Technol.* **1994**, *28*, 1300−1306.
(47) Dodge, C. J.; Francis, A. J. *Environ. Sci. Technol.* **2002**, *36*, 2094−2100.
(48) Francis, A. J.; Dodge, C. J.; Gillow, J. B. *Nature* **1992**, *356*, 140−142.
(49) Fairley, M.; Unruh, D. K.; Abeysinghe, S.; Forbes, T. Z. *Inorg. Chem.* **2012**, *51*, 9491−9498.
(50) Fairley, M.; Unruh, D. K.; Donovan, A.; Abeysinghe, S.; Forbes, T. Z. *Dalton Trans.* **2013**, *42* (37), 13706−13714.
(51) Hoft, R. W. W. *COLLECT*; Nonius BV: Delft, The Netherlands, 1998.
(52) Sheldrick, G. M. *APEX II*; Bruker AXS: Madison, WI, USA, 1996.
(53) Spek, A. L. *PLATON, A Multipurpose Crystallographic Tool*; Utrecht University: Utrecht, The Netherlands, 2005.
(54) Takao, S.; Takao, K.; Kraus, W.; Emmerling, F.; Scheinost, A. C.; Bernhard, G.; Hennig, C. *Eur. J. Inorg. Chem.* **2009**, *32*, 4771−4775.
(55) Hu, Y.-J.; Knope, K. E.; Skanthakumar, S.; Kanatzidis, M. G.; Mitchell, J. F.; Soderholm, L. *J. Am. Chem. Soc.* **2013**, *135*, 14240−14248.
(56) Neck, V.; Muller, R.; Bouby, M.; Altmaier, M.; Rothe, J.; Denecke, M. A.; Kim, J.-I. *Radiochim. Acta* **2002**, *90*, 485−494.
(57) Thuery, P. *Inorg. Chem.* **2011**, *50*, 1898−1904.
(58) Frisch, M.; Cahill, C. L. *Cryst. Growth Des.* **2008**, *8*, 2921−2928.
(59) Seichter, W.; Mogel, H.-J.; Brand, P.; Salah, D. *Eur. J. Inorg. Chem.* **1998**, 795−797.
(60) Gatlin, J. T.; Mensinger, Z. L.; Zakharov, L. N.; Macinnes, D.; Johnson, D. W. *Inorg. Chem.* **2008**, *47*, 1267−1269.
(61) Jordan, P. A.; Clayden, N. J.; Heath, S. L.; Moore, G. R.; Powell, A. K.; Tapparo, A. *Coord. Chem. Rev.* **1996**, *149*, 281−309.
(62) Heath, S. L.; Powell, A. K. *Angew. Chem., Int. Ed.* **1992**, *31*, 191−193.
(63) Murugesu, M.; Clerac, R.; Wernsdorfer, W.; Anson, C. E.; Powell, A. K. *Angew. Chem., Int. Ed.* **2005**, *44*, 6678−6682.
(64) Powell, A. K.; Heath, S. L.; Gatteschi, D.; Pardi, L.; Sessoli, R.; Spina, G.; Del Giallo, F.; Pieralli, F. *J. Am. Chem. Soc.* **1995**, *117*, 2491−2502.
(65) Schmitt, W.; Zhang, L.; Anson, C. E.; Powell, A. K. *Dalton Trans.* **2010**, *39*, 10279−10285.
(66) Bino, A.; Shweky, I.; Cohen, S.; Bauminger, E. R.; Lippard, S. J. *Inorg. Chem.* **1998**, *37*, 5168−5172.
(67) Torapava, N.; Radkevich, A.; Persson, I.; Davydov, D.; Eriksson, L. *Dalton Trans.* **2012**, *41*, 4451−4459.
(68) Stumm, W.; Wehrli, B.; Wieland, E. *Croat. Chem. Acta* **1987**, *60*, 429−456.
(69) Whitfield, M.; Turner, D. R. The role of particles in regulating the composition of seawater. In *Aquatic Surface Chemistry: Chemical Processses at the Particle-Water Interface*; Stumm, W., Ed. John Wiley and Sons: New York, NY, USA, 1987.
(70) Osthols, E. *Geochim. Cosmochim. Acta* **1995**, *59*, 1235−1249.
(71) Degueldre, C.; Kline, A. *Earth Planet. Sci. Lett.* **2007**, *264*, 104−113.
(72) Schmidt, M.; Lee, S. S.; Wilson, R. E.; Soderholm, L.; Fenter, P. *Geochim. Cosmochim. Acta* **2012**, *88*, 66−76.
(73) Seco, F.; Hennig, C.; De Pablo, J.; Rovira, M.; Rojo, I.; Marti, V.; Gimenez, J.; Duro, L.; Grive, M.; Bruno, J. *Environ. Sci. Technol.* **2009**, *43*, 2825−2830.

DOI: 10.1021/ic502313y
Inorg. Chem. 2015, 54, 1395−1404